

## Dynamics of confined monopoles and similarities with confined quarks

Gia Dvali, Juan Sebastián Valbuena-Bermúdez<sup>✉,\*</sup> and Michael Zantedeschi<sup>†</sup>

*Arnold Sommerfeld Center, Ludwig-Maximilians-Universität, Theresienstraße 37, 80333 München, Germany and Max-Planck-Institut für Physik, Föhringer Ring 6, 80805 München, Germany*

 (Received 5 November 2022; accepted 10 March 2023; published 7 April 2023)

In this work, we study the annihilation of a pair of 't Hooft-Polyakov monopoles due to confinement by a string. We analyze the regime in which the scales of monopoles and strings are comparable. We compute the spectrum of the emitted gravitational waves and find it to agree with the previously calculated pointlike case for wavelengths longer than the system width and before the collision. However, we observe that in a head-on collision, monopoles are never recreated. Correspondingly, not even once the string oscillates. Instead, the system decays into waves of Higgs and gauge fields. We explain this phenomenon by the loss of coherence in the annihilation process. Due to this, the entropy suppression makes the recreation of a monopole pair highly improbable. We argue that in a similar regime, analogous behavior is expected for the heavy quarks connected by a QCD string. There too, instead of restretching a long string after the first collapse, the system hadronizes and decays in a high multiplicity of mesons and glueballs. We discuss the implications of our results.

DOI: [10.1103/PhysRevD.107.076003](https://doi.org/10.1103/PhysRevD.107.076003)

### I. INTRODUCTION

It is well known [1–4] that monopoles carrying the opposite magnetic charges under a  $U(1)$  gauge symmetry become connected by a string when  $U(1)$  is Higgsed. The string represents a magnetic flux tube of Nielsen-Olesen type [5]. As long as the mass of the monopole is larger than the scale of the string tension, energy per unit length  $\mu$ , the breakup of the string via nucleation of monopole pairs is exponentially unlikely [3].

This system shares some similarity with a quark–antiquark pair connected by a QCD string in a confining gauge theory. The QCD string represents a flux tube of the color electric field. The string tension,  $\mu = \Lambda^2$ , is set by the QCD scale,  $\Lambda$ . As long as all quarks in the theory are heavier than  $\Lambda$ , the probability of breaking the string by a pair creation is exponentially small.

Due to this analogy, studying monopoles connected by a magnetic string can serve as a useful test-laboratory for understanding certain features of confined heavy quarks.

The above systems have a number of interesting applications in particle physics and cosmology.

For example, recently a novel mechanism for producing the primordial black holes was proposed in [6]. Therein, quark pairs, produced and diluted in the inflationary era, are confined in the late Universe. Upon horizon reentry, they collapse and form black holes (BHs) due to the large amount of energy stored in the flux tubes connecting them. Given the constant acceleration of quarks sourced by the string, gravitational waves (GWs) of frequency comparable to the inverse of the horizon size are produced. Analogous considerations could be applied to the case of confined monopoles [7].

Previous calculations of the radiated GW spectrum were performed by Martin and Vilenkin [8] in the pointlike approximation, in which the size of monopoles as well as the width of the string are set to zero. In this limit, they obtained the following emitted power for a large range of frequencies

$$P_n \sim \frac{\Lambda^4}{M_p^2} \frac{1}{n}, \quad (1)$$

$n$  being the frequency number,  $M_p$  the planck mass, and  $\Lambda$  the confining scale. This relation was derived considering a pair of monopoles connected by a string and is expected to be valid in the case of confined quarks too. Such sources could explain the recent hints of stochastic GW background obtained from pulsar timing arrays [9,10]. Moreover, given the flatness of the resulting energy density across several orders of frequency [11], in the future, it will be possible to cross-check with other gravitational wave detectors sensitive to the lengths shorter than the pulsar timing arrays.

\*[juanv@mpp.mpg.de](mailto:juanv@mpp.mpg.de)  
†[michaelz@mpp.mpg.de](mailto:michaelz@mpp.mpg.de)

*Published by the American Physical Society under the terms of the Creative Commons Attribution 4.0 International license. Further distribution of this work must maintain attribution to the author(s) and the published article's title, journal citation, and DOI. Funded by SCOAP<sup>3</sup>.*

Another scenario for which our study is relevant is the Langacker-Pi mechanism [1]. In an attempt to solve the monopole abundance problem, the theory ensures a temporary (thermal) window in which the  $U(1)$  group associated to the monopole charge is broken, leading to their confinement.

At lower temperatures the  $U(1)$  symmetry is restored again. This mechanism can be achieved by adequately choosing the spectrum and couplings of the theory [12]. The system therefore has a finite window of opportunity for getting rid of monopoles. If monopoles connected by string can oscillate for too long, this window of opportunity is insufficient for solving the monopole problem [13,14].

The goal of the present work is to analyze the dynamics of a monopole/antimonopole pair in the confined phase in detail. In order to do so, we considered a  $SU(2)$  gauge theory and chose a simple scalar sector capable of achieving the above-mentioned configuration via spontaneous symmetry breaking: a scalar field in the adjoint representation, and a complex scalar doublet. The former breaks (Higgses) the gauge group  $SU(2)$  to  $U(1)$ , therefore admitting 't Hooft-Polyakov monopoles as a solution [15,16]. The latter breaks the residual  $U(1)$  gauge group leading to the confinement of the associated “magnetic flux.” Our study covers the regime in which the monopole size and the string width are comparable. The similarities with confined quarks are established in the analogous regime.

It turns out that the pointlike limit approximates very well the part of the classical dynamics in which the monopole separation is much larger than the characteristic width of the system. However, beyond this regime we observe some new features.

Naively, it is expected that a collapsing straight string performs several oscillations. That is, one would think that after shrinking, the end points (monopoles) scatter and fly apart stretching a long string again. In this way, the string would contract and expand with certain periodicity, as some sort of a rubber band.

However, we observe that in head-on collision the outcome is very different. After the first shrinkage the string never recovers. Instead, the entire energy is converted into the waves of Higgs and gauge particles. These waves can also be thought of as large number of overlapping short strings.

We explain this phenomenon and argue that in analogous kinematic regime the similar effect takes place in case of confined quarks. In this particular regime, in both cases, the outcome can be understood as the result of the entropy suppression for production of a highly coherent state in a collision process [17]. Due to this, instead of stretching a long string, the system prefers to produce many particles (short strings) which have a much higher entropy. In case of QCD, the collapse of a long string results into a high multiplicity of glueballs (closed strings) and mesons (open strings).

We also point out that inability of monopole and antimonopole to go through each other, falls in the same category as the suppression of the passage of a magnetic monopole through a domain wall, studied in [18]. In that example, the domain wall provides a support base for unwinding the monopole, similar to the role of the antimonopole in the present case. The recreation of the monopole state on the other side of the wall is unlikely due to the insufficiency of the microstate entropy of the monopole for overcoming the exponential suppression of the corresponding multiparticle amplitude [17]. This leads to the “erasure” of monopoles by domain walls. In [18], this mechanism was used to solve the cosmological monopole problem in grand unified theories. However, the phenomenon of erasure is of broader fundamental interest. In particular, this is indicated by the similarities between the erasure processes of confined quarks and confined monopoles discussed in the present paper.

It emerges that in the studied regime, the processes of the collapse of the confined pairs in both theories are governed by the same universal effect: the exponential suppression of production of a high occupation number (coherent) state, albeit of insufficient entropy [17].

The GW spectrum produced by confined monopoles is appropriately captured by the pointlike result for scales larger than the monopole width. As expected, we observe non-negligible corrections to the power spectrum for scales comparable to the monopole radius, where the emitted radiation is boosted, therefore providing corrections to the GWs emission produced by the confinement dynamics.

We expect that our results have implications for the collapse of the generic bounded strings such as the string-theoretic strings bounded by  $D$  branes [19,20].

The paper is organized as follows. First we discuss the system of confined monopoles and study it numerically. Next, we explain the underlying physics that is shared by confined quarks and monopoles. We then study emission of gravitational waves. Finally, we discuss sphalerons and give outlook and conclusions.

## II. SETUP

We will work with a  $SU(2)$  gauged field theory that contains a scalar field in the adjoint representation,  $\varphi^a$  ( $a = 1, 2, 3$ ), a scalar field in the fundamental representation,  $\psi$ , and gauge fields,  $W_\mu^a$ . The Lagrangian of the system is given by

$$\mathcal{L} = \frac{1}{2} D_\mu \varphi^a D^\mu \varphi^a + (D_\mu \psi)^\dagger D_\mu \psi - \frac{1}{4} W_{\mu\nu}^a W^{a\mu\nu} - V(\varphi, \psi), \quad (2)$$

where summation over repeated  $SU(2)$  indices is understood, and the field strengths for the gauge field is

$$W_{\mu\nu}^a = \partial_\mu W_\nu^a - \partial_\nu W_\mu^a + g\epsilon^{abc}W_\mu^b W_\nu^c. \quad (3)$$

The covariant derivatives are defined as

$$D_\mu \varphi^a = \partial_\mu \varphi^a + g\epsilon^{abc}W_\mu^b \varphi^c, \quad (4)$$

$$D_\mu \psi = \partial_\mu \psi - ig \frac{\sigma^a}{2} W_\mu^a \psi, \quad (5)$$

and the potential is given by [21]

$$V(\varphi, \psi) = \frac{\lambda}{4}(\varphi^a \varphi^a - \eta^2)^2 + \frac{\tilde{\lambda}}{2}(\psi^\dagger \psi - v^2)^2 + c\psi^\dagger \sigma^a \psi \varphi^a. \quad (6)$$

As the first stage of symmetry breaking, we give vacuum expectation value to the adjoint field while keeping  $\psi = 0$ . The system admits 't Hooft-Polyakov monopoles [16,22]. As  $\psi$  acquires vacuum expectation value, the residual  $U(1)$  gauge symmetry is Higgsed, and the magnetic flux of a monopole is trapped into a tube which can end on an antimonopole. In this way, monopoles become confined. The dynamics of such configuration are the main focus of this work. The initial configuration utilized in this work is sketched in Fig. 1. The monopoles are aligned along the  $z$  axis at a distance  $d$ . In the figure  $\theta$  and  $\bar{\theta}$  denote the respective monopole and antimonopole position azimuthal angle. In the approximation when the distance  $d$  is much longer than the monopole size the string configuration can be derived as follows. For  $\bar{\theta} = 0$ , a monopole should be recovered  $\psi \propto (\cos \theta/2, \sin \theta/2 e^{i\phi})^t$  [23,24], while for  $\theta = \pi$  an antimonopole should be obtained  $\psi \propto (\sin \bar{\theta}/2, \cos \bar{\theta}/2 e^{i\phi})^t$ ,  $\phi$  being the polar angle. Therefore, the string configuration is given by [25–27]

$$\psi \propto \begin{pmatrix} \sin(\theta/2) \sin(\bar{\theta}/2) e^{i\gamma} + \cos(\theta/2) \cos(\bar{\theta}/2) \\ \sin(\theta/2) \cos(\bar{\theta}/2) e^{i\phi} - \cos(\theta/2) \sin(\bar{\theta}/2) e^{i(\phi-\gamma)} \end{pmatrix} \quad (7)$$

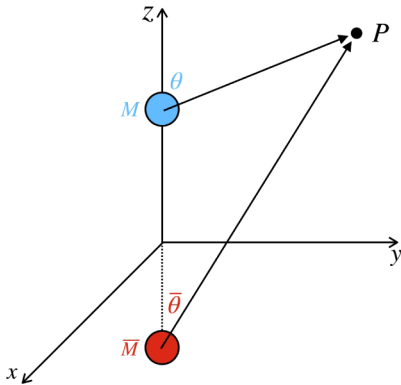


FIG. 1. A sketch of the initial monopole/antimonopole initial configuration.

with  $\gamma$  accounting for the possibility of twisting the antimonopole with respect to the monopole. In fact, for  $\theta = \pi$ ,  $\psi$  corresponds to the above-mentioned antimonopole under the shift  $\phi \rightarrow \phi + \gamma$ . Above the configuration, for  $\theta = \bar{\theta} = 0$ ,  $\psi = (v, 0)^t$ , while below  $\theta = \bar{\theta} = \pi$ ,  $\psi = (v e^{i\gamma}, 0)^t$ . Finally between the two monopoles,  $\theta = \pi$  and  $\bar{\theta} = 0$ ,  $\psi \propto (e^{i\phi}, 0)^t$  corresponding to the unit winding string.

Asymptotically the string is proportional to the positive eigenvector of the third Pauli matrix. Since we choose  $c < 0$  in the last term of the potential (6), the adjoint field direction  $\hat{\varphi}^a$  of the monopoles can be built asymptotically as [23,24]

$$\hat{\varphi}^a = \frac{1}{v^2} \psi^\dagger \tau^a \psi, \quad a = 1, 2, 3, \quad (8)$$

where  $\tau^a$  denotes the three Pauli matrices (see Fig. 2).

In the next section we analyze the monopole/antimonopole configuration after the first phase transition, ignoring the doublet. Although this was already explored by Vachaspati and Saurabh [26,27], it serves as a useful exercise before turning to the symmetry broken phase.

### III. MONOPOLE/ANTIMONOPOLE SYSTEM

The explicit equations of motion can be found in Appendix. From now, we work in energy units of  $\eta^{-1}$  and set the gauge coupling  $g = 1$ . Thus  $\lambda$  is the parameter in the theory that controls the mass and size of the monopoles.

For a (spherically symmetric) monopole field configuration, we use the following ansatz:

$$\varphi^a = h(r) \hat{r}^a, \quad W_i^a = \frac{(1-k(r))}{r} \epsilon^{aij} \hat{r}^j, \quad (9)$$

where  $r$  is the radial coordinate and  $\hat{r}^a = r^a/|\vec{r}|$ . Under ansatz (9), the equations of motion become

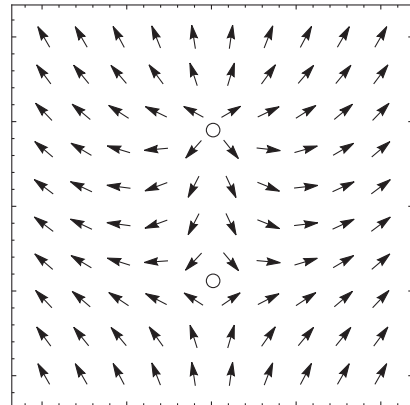


FIG. 2. Example of field configuration  $\hat{\varphi}^a$  for twist  $\gamma = 0$  according to Eq. (14) in the  $yz$  plane. The circles denote the position of the monopole and antimonopole.

$$h''(r) + \frac{2}{r}h'(r) = \frac{2}{r^2}k(r)^2h(r) - \lambda(h(r)^2 - 1)h(r), \quad (10)$$

$$k''(r) = \frac{1}{r^2}(k(r)^2 - 1)k(r) + h(r)^2k(r), \quad (11)$$

with asymptotic conditions

$$h(r) \xrightarrow{r \rightarrow 0} 0, \quad k(r) \xrightarrow{r \rightarrow 0} 1, \quad (12)$$

$$h(r) \xrightarrow{r \rightarrow \infty} 1, \quad k(r) \xrightarrow{r \rightarrow \infty} 0. \quad (13)$$

The above equations were solved numerically in order to obtain the monopoles profile.

Finally the ansatz for the initial adjoint field configuration is given by

$$\varphi^a = h(r_m)h(\bar{r}_m)\hat{\varphi}^a, \quad (14)$$

with  $r_m$  ( $\bar{r}_m$ ) denoting the monopole (antimonopole) coordinate center and  $\hat{\varphi}^a$  is defined in (8). An example of such configuration is shown in Fig. 2.

The stationary ansatz for the gauge fields considered by Vachaspati and Saurabh [26,27], follows from the requirement that the covariant derivative of the Higgs isovector vanish at spatial infinity,  $D_\mu \hat{\varphi}|_{r \rightarrow \infty} = 0$ . This gives

$$W_\mu^a = -(1 - k(r_m))(1 - k(\bar{r}_m))e^{abc}\hat{\varphi}^b\partial_\mu\hat{\varphi}^c. \quad (15)$$

As expected, and verified in [27], the monopole/antimonopole are attracted to each other due to a “magnetic” Coulomb-like interaction (for distances much bigger than the monopole size). Moreover, the potential energy is also affected by the initial system twist parametrized by  $\gamma$  [28]—such a correction, however, is exponentially suppressed at large distances. The verification of these properties served as a valuable check of the numerics presented in this work.

#### IV. MONOPOLE/ANTIMONOPOLE CONNECTED BY STRINGS

We solve field equations (A1)–(A4), with an initial configuration of the monopole/antimonopole given by (14) and (15). Before starting the dynamical evolution a numerical relaxation of the configuration was performed (cf. [27]).

Asymptotically  $\varphi^a = \eta\delta^{a3}$ , implying that  $\psi$ , due to the last interaction term in (6), needs to be proportional to the positive  $\sigma^3$  eigenvector  $\langle |\psi| \rangle \propto (1, 0)^t$ , as correctly implied by ansatz (7).<sup>1</sup>

Above the pair,  $\psi$  ansatz minimizes the interaction energy. As it crosses the monopole, the configuration

becomes singular at the south pole and its phase is flipped by  $2\pi$ . It follows that between the two monopoles, along the axial axes,  $\psi \propto (0, e^{i\phi})^t$ ,  $\phi$  being the polar angle. By construction the associated winding number is one. Finally, as it reaches the antimonopole, the string flips by  $2\pi$  again and it becomes proportional to  $\psi \propto (e^{i\gamma}, 0)^t$ . While minimization of scalar potential is independent on the value of  $\gamma$ , the same is not true for both the kinetic terms and the gauge sector. In fact,  $\gamma \neq 0$  generates a repulsive interaction [27] between the quark/antiquark pair which can be easily shown to be maximal for  $\gamma = \pi$ . Unless otherwise stated, from now on we will focus on the case  $\gamma = 0$ .

As the magnetic field of the pair is confined into tubes, the monopoles accelerate towards each other, turning rapidly, relativistic and annihilate. In Fig. 3, snapshots of the time evolution of the magnetic field norm are shown. The string formation is observed at early times. For another visual representation of the collapse dynamics see the following link (the sphaleron dynamics described below is also shown there).

Effectively, the system behaves as a type II superconductor and the magnetic field is neutralized by the

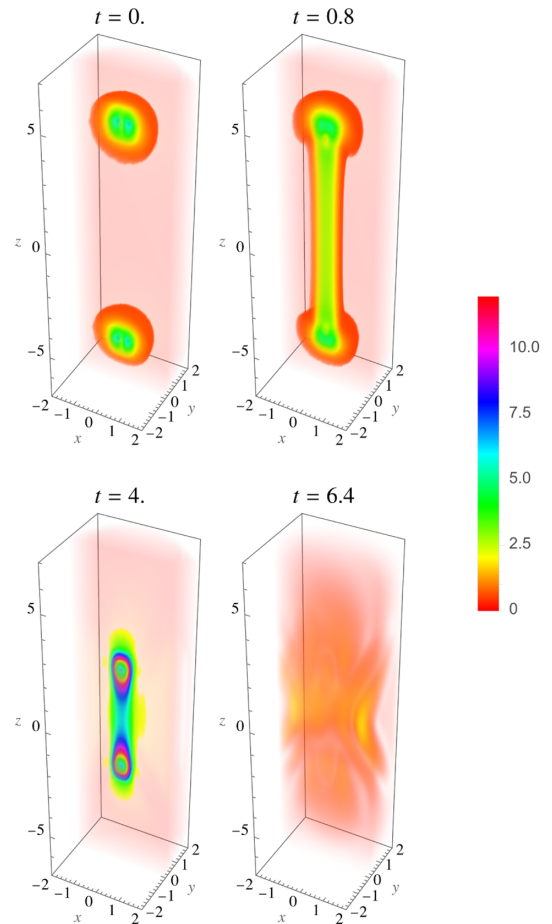


FIG. 3. Evolution of the magnetic field norm. The picture is sliced at  $y = 0$  for better readability.

<sup>1</sup>We used  $c < 0$  in our numerical simulations.



longitudinal massive photon component which is nothing but the eaten up Goldstone boson. Due to the compactness of the group, as expected, no residual magnetic field is observed. The confining string, being related to the breaking of the  $U(1)$  subgroup, carries the same magnetic flux as the original monopoles and is therefore able to fully neutralize the magnetic field.

An example of string formation is shown in Fig. 7, where the initial phase of  $\psi$  was randomly chosen at each lattice point. The emergence of the winding further justifies the chosen initial conditions mentioned at the beginning of this section, which is adopted from here onward.

The dynamics is well approximated by the pointlike study of Martin and Vilenkin [8]. The system they considered has action

$$I = -m_m \int ds_1 - m_m \int ds_2 - \Lambda^2 \int dS, \quad (16)$$

where the first two terms correspond to the monopole/antimonopole worldline, while the last term describes the string world sheet for Nambu action [24]. The equation of motion obtained by varying action (16) admits a particular solution of an exactly straight string with the monopole/antimonopole pair accelerating towards its center. Their trajectories are given by [8]

$$x(t) = \pm \frac{\text{sgn}(t)}{a} \left( \gamma_0 - \sqrt{1 + (\gamma_0 v_0 - a|t|)^2} \right), \quad (17)$$

where  $t_0 = -\gamma_0 v_0/a$ ,  $a = \Lambda^2/m_m$ ,  $v_0$  and  $\gamma_0 = (1 - v_0^2)^{-1/2}$  are, respectively, the maximum velocity and Lorentz factor of the monopoles, reached at  $t = 0$ .

As shown in Fig. 4, the trajectory followed by the centers of the monopoles (black dots) are nicely fitted by solution (17) (dashed line). As expected, the monopoles, due to the constant acceleration, rapidly become relativistic. However, differently from the pointlike solution, they annihilate upon reaching approximately zero distance. In contrast,

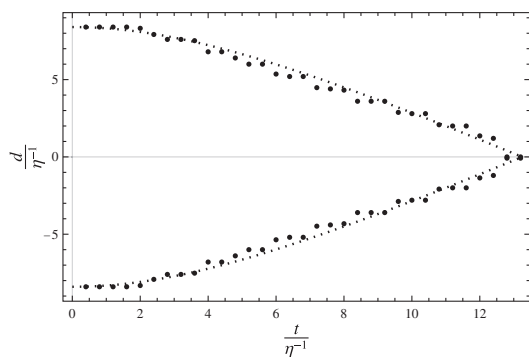


FIG. 4. Time evolution of the position of the cores of the monopole and antimonopole. The dots are numerical results while the dashed line is the pointlike solution (17). Here  $a = \mu/m_m = 0.16\eta$ .

in solution (17), they simply pass through each other and oscillate.

## V. SIMILARITIES BETWEEN CONFINED QUARKS AND MONOPOLES

Our numerical analysis shows that after the first direct collision, the monopole and antimonopole always annihilate and decay into waves without further oscillations.

First of all, we would like to notice that, in the Coulomb phase, the annihilation of monopoles and antimonopoles was also observed by Vachaspati in [26]. However, in that analysis, the scattering takes place at quite mild relativistic velocities, therefore leading to a rather prolonged overlapping between the two cores. In this sense, it is unsurprising that the monopoles can easily unwind.

In the present case, the process is ultra-relativistic and occurs at center-of-mass energies much higher than the mass of the two monopoles. Therefore, the observed annihilation might seem counterintuitive, since *a priori*, there is no reason for monopole and antimonopole not to pass through each other, stretching the string of the opposite polarity.

This phenomenon can be explained by the loss of coherence or, equivalently, by entropy suppression. The basic point is that once the monopole and antimonopole come on top of each other, the system loses coherence due to the emission of waves. A further re-creation of the monopole-antimonopole pair connected by a string represents a process of a transition from a highly energetic localized source into a coherent state of many soft quanta. Very general arguments [17] indicate that such a process is exponentially suppressed unless the microstate entropy of the coherent state is close to saturating a certain upper bound set by unitarity.

In the present case, the microstate degeneracy of the coherent state describing the pair of confined monopoles is not even close to this value.

Due to this, it is insufficient for matching the phase space occupied by the waves of Higgs and gauge bosons. Correspondingly, rather than creating a highly coherent configuration of monopoles confined by a long string with a much higher probability, the system chooses to decay into those waves.

Interestingly, the reasoning of [17] indicates that, in the analogous regime, a similar behavior is expected for the quarks confined by a long QCD string.

In order to display the arguments in the language applicable to both systems, let us consider a  $SU(N_c)$  gauge theory with a heavy quark transforming in a fundamental representation. The term “heavy” implies that the mass of the quark,  $m_q$ , is higher than the QCD scale,  $\Lambda$ . No light quarks are assumed to exist in the theory. The spin of the quark is not important for our analysis.

The scale  $\Lambda$  sets the boundary between the two descriptions. At distances shorter than the QCD length,  $\Lambda^{-1}$ , the

viable degrees of freedom are gluons and quarks. At distances larger than  $\Lambda^{-1}$ , the theory confines and the physical degrees of freedom are colorless composites such as glueballs and mesons.

The phenomenon of confinement is often described as a dual version of the Meissner effect [22,23,29]. The essence of this description is that the gluon “electric” field gets trapped in a flux tube when sources are separated by a distance  $d \gg \Lambda^{-1}$ . This is analogous to the behavior of the magnetic field of monopoles in the  $U(1)$ -Higgs phase. In the present discussion, the role of the sources will be played by a heavy quark-antiquark pair. When separated by a distance  $d \gg \Lambda^{-1}$ , the pair is connected by a QCD string. The thickness of the string is set by the QCD length  $\Lambda^{-1}$ . The string’s tension is given by the QCD scale,  $\mu \sim \Lambda^2$ .

Thus, a quark–antiquark pair connected by a QCD string is strikingly similar to a monopole–antimonopole connected by a magnetic flux tube. It is a long-standing question of how much of QCD physics is captured by this analogy.

In the processes in which the string stays longer than its thickness, the similarity between the two systems is not surprising. Naively, this similarity is not expected to extend to the processes in which the string shrinks to the size of its thickness, since physics governing the two systems at such distances are very different:

- (i) In the case of confined monopoles, the gauge theory is in the Higgs phase. The degrees of freedom are gauge and Higgs bosons. The monopoles, as well as the string connecting them, represent the solitonic objects.
- (ii) On the other hand, in QCD the quarks are fundamental particles rather than solitons. Also, the color string connecting them is not describable as a solitonic solution of the classical equations of motion.

Despite these differences, we can find out that the two systems do exhibit similarities even in certain processes controlled by physics below and around the scale  $\Lambda^{-1}$ .

This similarity concerns the observation in our numerical analysis that in a head-on collision the recreation of a long string never takes place. This behavior is expected to be shared by the confined quarks in the similar kinematic regime. Below we give supporting arguments. Our discussion will be mostly qualitative. In order to keep close to the parameters of our numerical analysis, we shall assume that  $m_q \sim \Lambda$ . Of course, we must assume that quark masses are somewhat larger than  $\Lambda$  in order for the long string to be sufficiently stable against the quantum break-up via pair nucleation. The system then is characterized by the two scales:  $\Lambda$  and the initial separation of quarks,  $d$ .

A useful physical way for understanding the suppression is via describing the string-formation process in an effective theory of glueballs and mesons. As said, these represent the correct physical degrees of freedom at distances larger than

the QCD length. In our parameter regime, the characteristic size of an unexcited glueball or a meson is  $\Lambda^{-1}$ , and their masses are  $\sim \Lambda$ .

Qualitatively, one can think of glueballs and mesons as of closed and open strings of sizes  $\Lambda^{-1}$ . We must however remember that such strings cannot be described as classical solitons. For this, it suffices to notice that the Compton wavelengths of glueballs and mesons are  $\sim \Lambda^{-1}$ . We shall assume that the initial energy is dominated by the energy of the string, and that the contributions from the quark masses are subdominant. That is,  $d \gg 1/m_q \sim \Lambda^{-1}$ . This implies that in the moment of the collision the quarks are ultrarelativistic.

The string that is shrunk to the size of its width  $\Lambda^{-1}$ , represents a blob of energy  $\sim d\Lambda^2$ . The energy per volume of quark Compton wavelength, is much larger than the masses of quarks. Correspondingly, quarks are effectively massless. Of course, the energy density is also much larger than the masses of unexcited mesons and glueballs. Correspondingly, the shrunk string is free to produce mesons and glueballs of high multiplicity,  $n \sim d\Lambda$ .

Thus, the system has to decide whether to produce a single long string or to hadronize into  $n$  short strings, in the form of the glueballs and mesons. The outcome is decided by the entropy of the final state. This entropy, in the case of a long string, is much less than the entropy of a generic state with high multiplicity of mesons and glueballs.

This can be understood from the fact that in an effective theory of glueballs and mesons, a long QCD string represents a coherent state. For  $d \gg \Lambda^{-1}$ , such a state can be viewed as approximately classical. The mean occupation number of its constituents can be estimated as

$$n \sim d\Lambda. \quad (18)$$

Their characteristic de Broglie wavelengths are given by  $\sim d$ . Now, it is intuitively clear that from all possible microstates of  $n$  mesons and glueballs, only a small fraction represents a highly coherent state of a long string. Correspondingly, the phase space for string formation is tiny.

For a better estimate, let us follow the scattering process more closely. When the initial string of size  $d$  collapses to the size  $\Lambda^{-1}$ , it can be viewed as a highly excited state of a meson. In this language a further formation of a long string represents a transition process from a highly energetic quantum meson into a coherent state of  $n$  soft quanta. According to [17], the probability of such a transition process is suppressed by the following universal factor,

$$\sigma \lesssim e^{-n+S}. \quad (19)$$

The first term  $e^{-n}$  encodes an exponential suppression characteristic of the transitions from a single particle state into a state of high occupation number  $n$ . The second factor,

$e^S$ , comes from the microstate entropy  $S$  of the final  $n$ -particle state. Not surprisingly, the entropy enhances the transition probability as it counts the number of the available final states.

In the present case, the final macrostate we are looking for is a QCD string of length  $d$ . For such a string, the degenerate microstates are given by all possible distinct orientations. Their number is  $\sim(d\Lambda)^2$  and the corresponding microstate entropy is given by,

$$S \sim \ln(d^2\Lambda^2). \quad (20)$$

Taking into account (18), we obtain the following estimate for the suppression factor

$$\sigma \lesssim e^{-d\Lambda+2\ln(d\Lambda)}. \quad (21)$$

This exponentially small number explains why in head-on collisions the system prefers to hadronize in a high multiplicity of short strings, rather than to produce a single long one.

In other words, due to insufficient entropy, a long QCD string cannot saturate the transition process from a highly energetic meson state. As argued in [17], for an unsuppressed production of an  $n$ -particle coherent state in a transition process of the type,  $1 \rightarrow n$ , its microstate entropy must be  $S \simeq n$ . This is clear from Eq. (19). The states with such a high entropy were referred to as ‘‘saturons.’’ The expression (20) shows that the entropy of the long string is much less than the saturation entropy. This is the main reason for the suppression. Since the production of a long string is exponentially suppressed, the system fills the remaining phase space by a hadronization into a high multiplicity of mesons and glueballs.

Physics that governs dynamics in the similar kinematic process with monopoles is analogous. After the collapse of a long string, the system forms a blob with very high energy density. It is entropically preferred to dissipate this energy in high multiplicity of Higgs and gauge bosons rather than in a highly coherent state of monopoles connected by a long string.

Thus, the suppression of the monopoles-passage through each other, as well as the inability of self-recreation of a long QCD string after its fist collapse, represent the phenomena belonging to the same universality class of effects taking place in high energy collisions. Their unifying feature is the exponential suppression of production of coherent states with insufficient microstate entropy [17].

Another phenomenon belonging to the same universality class is the inability of a monopole to go through a domain wall, discussed in [18]. In this theory, the domain wall represents a two-dimensional sheet in which the Higgs field vanishes and the non-Abelian (grand unification) symmetry is restored. Due to this, when a monopole meets the wall, it is no longer subject to the topological obstruction

that keeps the entire magnetic charge in one point. Correspondingly, the monopole unwinds and the magnetic charge is spread along the wall.<sup>2</sup>

In [18] this effect was called the ‘‘erasure’’ of topological defects. It was argued that, as a bonus, this mechanism can substantially reduce the cosmological abundance of monopoles in grand unified theories. In such theories the phase transition that forms monopoles, at the same time, forms the unstable domain walls. The walls sweep away monopoles and then disappear. A somewhat analogous effect of erasure was observed in  $2 + 1$  dimensions in interactions between skyrmions and domain walls [31], and, more recently, between vortices and domain walls [32].

Although it is both energetically and topologically permitted for the monopole (or a skyrmion) to go through the wall and materialize on the other side, the process is highly unlikely. This is also confirmed by more recent numerical analysis of the monopole-wall system [33]. Again, the reason is the loss of coherence and the entropy suppression. In the example of [18], the domain wall provides a support for unwinding the magnetic charge in the same way as the antimonopole does in the present case. The loss of coherence due to induced waves makes the recreation of monopole configuration improbable.<sup>3</sup>

We expect that a similar entropy reasoning can be applicable also for the scattering of a monopole-antimonopole pair in the Coulomb phase both in the regime considered in [26], as well as at ultrarelativistic energies. However, in these regimes, there exists no confining string of comparable width that would contribute to the entropy count, cf. (21). The entropies that must be confronted are the entropy of free waves versus the entropy of the monopole-antimonopole pair. In a mildly relativistic regime, it is natural that the entropy of a monopole pair is subdominant, and thereby annihilation is expected with a high probability. This matches the result of [26]. However, the regime of the ultrarelativistic Coulomb case requires a separate study.

From the point of view of Ref. [17], all the considered cases fall in the universal category of the processes in which

<sup>2</sup>Of course, within specific grand unified models, there can exist monopoles that are not affected topologically by a given domain wall and thereby can pass through without spreading the magnetic charge [30]. These are not relevant for the present discussion.

<sup>3</sup>In this respect, it is interesting to compare the situation with scattering of solitons in  $1 + 1$  dimensional theory, which are known to be able to go through each other [34]. There are at least two factors that make difference with the monopole case. First is dimensionality which restricts the phase space for the loss of coherence. Unlike monopoles, in case of kinks there is no transverse direction available for emitting the waves. Correspondingly, the precursors that could potentially take away coherence can only travel in the same directions as kinks and cannot escape efficiently. The second factor is confinement. It will be interesting to study the system within our parameter space. We thank Tanmay Vachaspati for raising this question.

the microstate entropy of the final coherent state is not sufficient for compensating the exponential suppression (19). As discussed, the same conclusion applies to a long QCD string viewed as a coherent state in the effective theory of mesons and glueballs.

This said, one can certainly imagine the parameter regimes in which the long string can be recreated with less suppression. For example, let us assume  $m_q \gg \Lambda$  and the energy of the initial string  $= 3m_q$ . In such a case, the quark–antiquark pair moving apart after the first collision, can stretch a string of the length  $d \sim m_q/\Lambda^2$ . This is because the system does not possess the energy required for creating an additional quark–antiquark pair, necessary for the string breakup. Of course, even in this regime, quarks can annihilate into gluons which then will hadronize, without recreating a long string. However, the annihilation cross section is perturbative since the scattering length is much shorter than  $\Lambda^{-1}$ .

Also, in the case of monopoles, behavior can be very different in the regime where the monopole size is much smaller than the string’s width. In this situation, for the nonzero impact parameter, the monopole and antimonopole can miss each other, and the string can oscillate, while shrinking to the size of its width. One may expect that the efficiency of annihilation requires that the impact parameter is less than the size of the monopole core. In this case, the annihilation cross section presumably will be suppressed by a geometric factor.<sup>4</sup> However, the understanding of this regime requires a separate study.

## VI. GRAVITATIONAL WAVES

The radiated power at frequency  $\omega_n = 2\pi n/T$  ( $T$  being the collapse time),<sup>5</sup> per unit solid angle in the direction  $\mathbf{k}$ ,  $|\mathbf{k}| = \omega_n$  can be computed as [35]

$$P = \sum_n P_n = \sum_n \int d\Omega \frac{dP_n}{d\Omega},$$

$$\frac{dP_n}{d\Omega} = \frac{G\omega_n^2}{\pi} \left( T_{\mu\nu}^*(\omega_n, \mathbf{k}) T^{\mu\nu}(\omega_n, \mathbf{k}) - \frac{1}{2} |T_\mu^\mu(\omega_n, \mathbf{k})|^2 \right), \quad (22)$$

where the energy-momentum tensor in momentum space is given by

$$T^{\mu\nu}(\omega_n, \mathbf{k}) = \frac{1}{T} \int_0^T dt e^{i\omega_n t} \int d^3\mathbf{x} e^{-i\mathbf{k}\cdot\mathbf{x}} T^{\mu\nu}(t, \mathbf{x}). \quad (23)$$

The radiated spectrum obtained from our simulation is shown in Fig. 5, where the dependence of  $(P_n \cdot n)$  vs  $n$  is

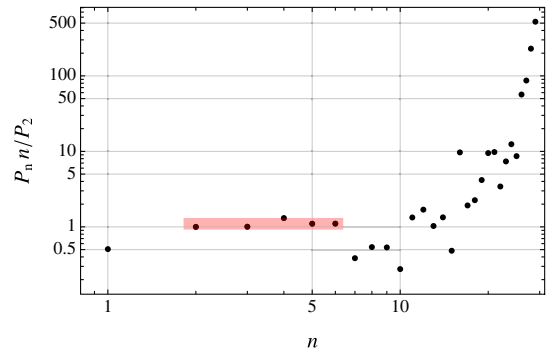


FIG. 5. Angularly integrated power emitted  $P_n$  according to (22). The amplitude was normalized with respect to the lowest frequency comparable to the initial distance between monopole and antimonopole, up to frequencies comparable to the monopoles size  $P_n \propto n^{-1}$  (shaded region).

shown over logarithmic intervals. We normalised the plot with respect to  $P_2$ , corresponding to a wavelength comparable to half of the monopoles initial distance. Direct comparison with the pointlike study of Martin and Vilenkin [8] shows interesting salient features.

As expected, for low frequencies,  $n \lesssim 7$  (red shaded area in the plot), corresponding to an emitted radiation when the monopoles are still far from each other, our result is well approximated by the pointlike study. In fact, a spectrum behavior  $P_n \propto n^{-1}$  is observed similar to the pointlike case [8]. However, the spectrum is different when the monopoles annihilate. In fact, as shown in Fig. 5 the monopole annihilation boosts the radiation spectrum for frequencies comparable to the monopoles and string width. Even though it was not possible to find an exact scaling of the spectrum in this region, this behavior is different from the pointlike case where no enhancement is observed.

The corrections to the spectrum of gravitational waves coming from the finite widths of the string and monopoles, can be of observational interest in cases when this length scale is macroscopic. For example, a string of the tension  $\mu = (10^{16} \text{ GeV})^2$  can have a width of order km, provided the gauge coupling of the theory is  $g \sim 10^{-35}$ . Existence of such superweak gauge interaction in some hidden sector of the theory is fully consistent with all known laws of physics. Of course, the parameters in our simulation could not be taken with such extreme values. However, the dynamic of the string can be significantly affected due to the difference of Higgs and magnetic cores as in the regimes discussed in [36]. Correspondingly, applications of our results for such parameter ranges, can only be viewed as indicative.

## VII. SPHALERON

So far we have been focused on the untwisted configuration, i.e.,  $\gamma = 0$ . This corresponds to a minimum of the string energy. While it is obvious from (7) that rotating  $\gamma$  by

<sup>4</sup>We thank Alex Vilenkin for commenting.

<sup>5</sup>For practical purposes we chose  $T = 2d\eta^{-1}$ ,  $d$  being the lattice distance between monopoles.



$2\pi$  gives back the same configuration, it is straightforward to see how the energy varies with  $\gamma$  (at fixed distance  $d$ ) and find that  $\gamma = \pi$  is an energy maximum.

The role of the twist  $\gamma$  has a deep topological meaning. There exists a static bound state configuration known as “sphaleron”—see, e.g., [37] for a review and [38–40] for solutions in the electroweak sector. This bounded configuration interpolates between vacua of different Chern-Simons number. It corresponds to the maximum of the noncontractible loop interpolating between two such minima and has Chern-Simons number  $1/2$  [39].

It was argued in [41] that such unstable solutions can be understood as a monopole and a rotated antimonopole. For the maximal twist  $\gamma = \pi$ , the Chern-Simons number of (15) corresponds to that of a sphaleron as it can be easily checked.

References [27,42] have numerically verified the behavior of this object in the unconfined case. They observed that the twist  $\gamma = \pi$  prevents the monopole-antimonopole annihilation. To our knowledge, the behavior of this configuration in the confined phase has not been studied so far.

In Fig. 6, the position of the two monopoles core centers is shown as a function of time. As it can be seen, at initial time the two magnetic cores start to accelerate towards each other due to the flux tubes connecting them, dragging the scalar core along and the system becomes relativistic.

The dynamics is analogous to the untwisted one, cf. Fig. 4, up to the collapse moment. While in the untwisted case the two monopoles annihilate right away, in the twisted case they do not. Instead, the magnetic cores repel each other, slow down and bounce back.

From there on the two monopoles have a bouncing behavior, and dissipate energy up to settling to a constant distance where the confining energy is balanced by the repulsive twist energy. Eventually, the pair fully annihilates. Concomitantly, a deviation from axial symmetry is observed. Given the axial symmetry of the initial configuration, and the fact that the dynamics should preserve such symmetry, we believe this to be a numerical artifact.

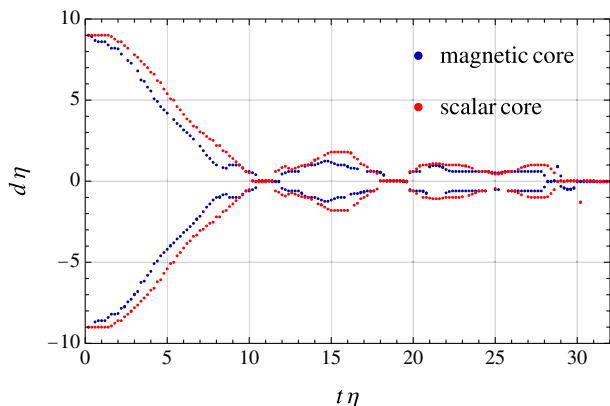


FIG. 6. Evolution of the magnetic and scalar cores of the monopole/antimonopole pair for initial twist  $\gamma = \pi$ .

In Fig. 6,  $\Lambda \simeq \eta$  was used. For lower value of this parameter the bouncing sizes, as well as distance of the bound state were observed to be larger. For a different initial distance, two-dimensional slices of the dynamics can be found at the following link.

For  $\gamma \neq \pi$ , no bounce is observed, as the system can always untwist in the direction of a favorable minimum, thereby annihilating right away.

## VIII. CONCLUSION AND OUTLOOK

In this article we numerically studied the confinement of a  $SU(2)$  monopole/antimonopole pair. Initially the pair is in a dipolar configuration as in Fig. 2. The confinement is instantaneously imposed by setting an extra complex doublet field in its Higgs phase, therefore breaking the residual  $U(1)$  and giving mass to the previously massless “photon.”

As shown in Fig. 4, very quickly the monopoles become relativistic due to confinement. Taking initial random phases for the confining scalar field, it is possible to see the dynamical emergence of the tube as shown in Fig. 7.

The GW spectrum is also computed and is compared with the pointlike study of Martin and Vilenkin [8]. Before the collision and for the wavelengths longer than the relevant widths of the system (i.e., monopoles and string width) we find perfect agreement. Namely, we confirm a power spectrum  $P_n \propto n^{-1}$ ,  $n$  denoting the frequency number. As previously mentioned, this type of spectrum can lead to a flat density of GWs  $\Omega_{\text{GW}}$  across several orders of the frequency, therefore making it interesting from a phenomenological perspective in view of future refinement of the stochastic GW background hints obtained from pulsar timing arrays [9,10].

However, in our parameter regime, in which the scales of string and monopoles are of the same order, we observe the following differences from the pointlike case.

Firstly, an enhancement of the GW spectrum for wavelengths comparable to the monopoles and string size as shown in Fig. 5, therefore providing finite-width corrections to the pointlike case [8]. This can be of phenomenological interest for the strings of a macroscopic width. Notice that such strings can have a high tension provided the gauge coupling is sufficiently weak and can produce intense gravitational waves.

Secondly, in our numerical analysis we have observed an interesting effect. After the first collision, the monopoles annihilate without any further oscillations. We gave a qualitative explanation to this observation in terms of a general phenomenon of suppressed production of low-entropy coherent states in a collision process [17]. In the present case, the loss of coherence in the monopole-antimonopole collision, makes the recreation of a monopole-string system unlikely due to an insufficient entropy of such a state.

Applying the general reasoning of [17], we argued that in the similar parameter regime this behavior must be shared by heavy quarks confined by a long QCD string. There too,

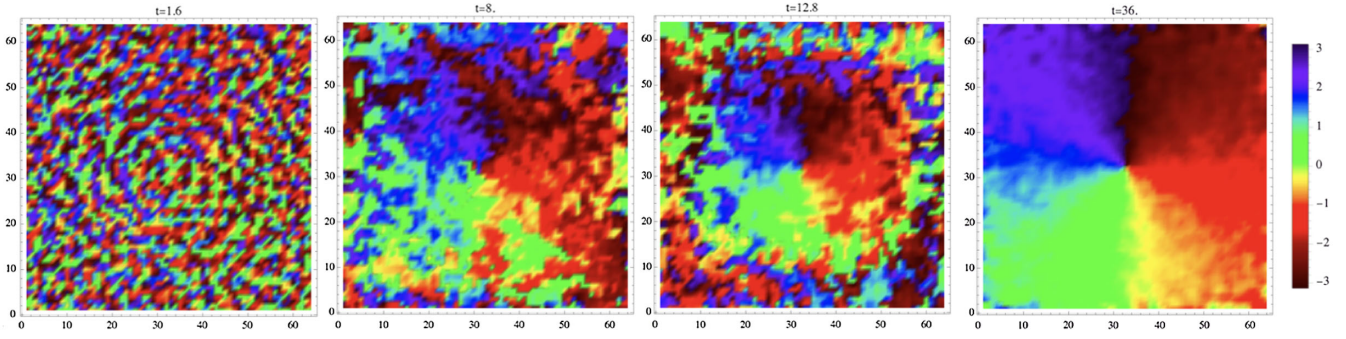


FIG. 7. Phase of the confining scalar field in the  $xy$  plane at the middle of the string height.

after the collapse of a straight long string, instead of restretching it in an oscillatory mode, the system prefers to directly decay into high multiplicity of mesons and glueballs. This similarity extends the connection between the confined quarks and monopoles to the domain of processes controlled by the short-distance physics.

### ACKNOWLEDGMENTS

We thank Tanmay Vachaspati and Alex Vilenkin for useful discussions and valuable comments. This work was supported in part by the Humboldt Foundation under the Humboldt Professorship Award, by the Deutsche Forschungsgemeinschaft (DFG, German Research Foundation) under Germany's Excellence Strategy—EXC-2111-390814868, and Germany's Excellence Strategy under Excellence Cluster Origins.

### APPENDIX: FIELDS EQUATION

#### 1. Field equations

The field equations can be written as

$$\begin{aligned} \partial_t^2 \varphi^a &= \nabla^2 \varphi^a - g\epsilon^{abc} \partial_i \phi^b W_i^c - g\epsilon^{abc} (D_i \varphi)^b W_i^c \\ &\quad - \lambda(\varphi^b \varphi^b - \eta^2) \varphi^a - g\epsilon^{abc} \varphi^b \Gamma^c - c\psi^\dagger \sigma^a \psi, \end{aligned} \quad (\text{A1})$$

$$\begin{aligned} \partial_t^2 \psi^\alpha &= \nabla^2 \psi^\alpha - \frac{g^2}{4} W_i^a W_i^a \psi^\alpha - i\frac{g}{2} \Gamma^a (\sigma^a \psi)^\alpha \\ &\quad - igW_i^a (\sigma^a \partial_i \psi)^\alpha - c\varphi^a \sigma^a \psi^\alpha - \tilde{\lambda}(\psi^\dagger \psi - v^2) \psi^\alpha, \end{aligned} \quad (\text{A2})$$

$$\begin{aligned} \partial_t W_{0i}^a &= \nabla^2 W_i^a + g\epsilon^{abc} W_j^b \partial_j W_i^c - g\epsilon^{abc} W_j^b W_{ij}^c - D_i \Gamma^a \\ &\quad - g\epsilon^{abc} \varphi^b (D_i \varphi)^c - \frac{1}{2} g^2 \psi^\dagger \psi W_i^a - ig\psi^\dagger \sigma^a \partial_i \psi, \end{aligned} \quad (\text{A3})$$

$$\begin{aligned} \partial_t \Gamma^a &= \partial_i W_{0i}^a - g_p^2 [\partial_i (W_{0i}^a) + g\epsilon^{abc} W_i^b W_{0i}^c \\ &\quad + g\epsilon^{abc} \varphi^b (D_i \varphi)^c + ig\psi^\dagger \sigma^a \partial_i \psi], \end{aligned} \quad (\text{A4})$$

where we are using the temporal gauge,  $W_0^a = 0$ ,  $\Gamma^a = \partial_i W_i^a$  are introduced as new variables, and  $g_p^2 = 1.5$  is a numerical parameter that we can choose to ensure numerical stability. The equations were evolved with a Crank-Nicolson leapfrog algorithm combined with absorbing boundary conditions [43].

- 
- [1] Paul Langacker and So-Young Pi, Magnetic Monopoles in Grand Unified Theories, *Phys. Rev. Lett.* **45**, 1 (1980).
  - [2] George Lazarides, Q. Shafi, and T. F. Walsh, Cosmic strings and domains in unified theories, *Nucl. Phys.* **B195**, 157 (1982).
  - [3] A. Vilenkin, cosmological evolution of monopoles connected by strings, *Nucl. Phys.* **B196**, 240 (1982).
  - [4] A. Vilenkin and E. P. S. Shellard, *Cosmic Strings and Other Topological Defects* (Cambridge University Press, Cambridge, England, 2000).
  - [5] Holger Bech Nielsen and P. Olesen, Vortex Line Models for Dual Strings, *Nucl. Phys.* **B61**, 45 (1973).
  - [6] Gia Dvali, Florian Kühnel, and Michael Zantedeschi, Primordial black holes from confinement, *Phys. Rev. D* **104**, 123507 (2021).
  - [7] Tomohiro Matsuda, Primordial black holes from monopoles connected by strings, *Astropart. Phys.* **30**, 333 (2009).
  - [8] Xavier Martin and Alexander Vilenkin, Gravitational radiation from monopoles connected by strings, *Phys. Rev. D* **55**, 6054 (1997).

- [9] Zaven Arzoumanian *et al.* (NANOGrav Collaboration), The NANOGrav 12.5 yr Data Set: Search for an isotropic stochastic gravitational-wave background, *Astrophys. J. Lett.* **905**, L34 (2020).
- [10] J. Antoniadis *et al.*, The International Pulsar Timing Array second data release: Search for an isotropic Gravitational Wave Background, *Mon. Not. R. Astron. Soc.* **510**, 4873 (2022).
- [11] Louis Leblond, Benjamin Shlaer, and Xavier Siemens, Gravitational waves from broken cosmic strings: The bursts and the beads, *Phys. Rev. D* **79**, 123519 (2009).
- [12] Steven Weinberg, Gauge and global symmetries at high temperature, *Phys. Rev. D* **9**, 3357 (1974).
- [13] Ya. B. Zeldovich and M. Yu. Khlopov, On the concentration of relic magnetic monopoles in the Universe, *Phys. Lett. B* **79**, 239 (1978).
- [14] J. Preskill, Cosmological Production of Superheavy Magnetic Monopoles, *Phys. Rev. Lett.* **43**, 1365 (1979).
- [15] G. 't Hooft, Magnetic monopoles in unified theories, *Nucl. Phys. B* **79**, 276 (1974).
- [16] Alexander M. Polyakov, Compact gauge fields and the infrared catastrophe, *Phys. Lett.* **59B**, 82 (1975).
- [17] Gia Dvali, Entropy bound and unitarity of scattering amplitudes, *J. High Energy Phys.* **03** (2021) 126.
- [18] G. R. Dvali, Hong Liu, and Tanmay Vachaspati, Sweeping Away the Monopole Problem, *Phys. Rev. Lett.* **80**, 2281 (1998).
- [19] Edmund J. Copeland, Robert C. Myers, and Joseph Polchinski, Cosmic F and D strings, *J. High Energy Phys.* **06** (2004) 013.
- [20] Gia Dvali and Alexander Vilenkin, Formation and evolution of cosmic D strings, *J. Cosmol. Astropart. Phys.* **03** (2004) 010.
- [21] T. W. B. Kibble and Tanmay Vachaspati, Monopoles on strings, *J. Phys. G* **42**, 094002 (2015).
- [22] Gerard 't Hooft, On the phase transition towards permanent quark confinement, *Nucl. Phys.* **B138**, 1 (1978).
- [23] Yoichiro Nambu, Strings, monopoles and gauge fields, *Phys. Rev. D* **10**, 4262 (1974).
- [24] Yoichiro Nambu, String-like configurations in the Weinberg-Salam theory, *Nucl. Phys.* **B130**, 505 (1977).
- [25] Tanmay Vachaspati and George B. Field, Electroweak String Configurations with Baryon Number, *Phys. Rev. Lett.* **73**, 373 (1994).
- [26] Tanmay Vachaspati, Monopole-antimonopole scattering, *Phys. Rev. D* **93**, 045008 (2016).
- [27] Ayush Saurabh and Tanmay Vachaspati, Monopole-antimonopole interaction potential, *Phys. Rev. D* **96**, 103536 (2017).
- [28] Clifford Henry Taubes, The existence of a nonminimal solution to the SU(2) Yang-Mills Higgs equations on  $\mathbb{R}^{**3}$ , *Commun. Math. Phys.* **86**, 257 (1982).
- [29] S. Mandelstam, Vortices and quark confinement in non-Abelian gauge theories, *Phys. Rep.* **23**, 245 (1976).
- [30] Micah Brush, Levon Pogosian, and Tanmay Vachaspati, Magnetic monopole—domain wall collisions, *Phys. Rev. D* **92**, 045008 (2015).
- [31] Alexander Evgenyevich Kudryavtsev, B. M. A. G. Piette, and W. J. Zakrzewski, Skyrmions and domain walls in  $(2 + 1)$ -dimensions, *Nonlinearity* **11**, 783 (1998).
- [32] G. Dvali and J. Valbuena-Bermúdez, Erasure of vortices, *Phys. Rev. D* **107**, 035001 (2023).
- [33] M. Bachmaier, G. Dvali, and J. Valbuena-Bermúdez, Radiation emission during the erasure of magnetic monopoles (to be published).
- [34] R. Rajaraman, *Solitons and Instantons. An Introduction to Solitons and Instantons in Quantum Field Theory* (North-Holland Publishing Company, 1982).
- [35] Steven Weinberg, *Gravitation and Cosmology: Principles and Applications of the General Theory of Relativity* (John Wiley and Sons, New York, 1972).
- [36] Eric Adelberger, Gia Dvali, and Andrei Gruzinov, Photon Mass Bound Destroyed by Vortices, *Phys. Rev. Lett.* **98**, 010402 (2007).
- [37] N. S. Manton and P. Sutcliffe, *Topological Solitons*, Cambridge Monographs on Mathematical Physics (Cambridge University Press, Cambridge, England, 2004).
- [38] Frans R. Klinkhamer and N. S. Manton, A saddle point solution in the Weinberg-Salam theory, *Phys. Rev. D* **30**, 2212 (1984).
- [39] N. S. Manton, Topology in the Weinberg-Salam theory, *Phys. Rev. D* **28**, 2019 (1983).
- [40] Yves Brihaye and Jutta Kunz, On axially symmetric solutions in the electroweak theory, *Phys. Rev. D* **50**, 4175 (1994).
- [41] Clifford Henry Taubes, The existence of a nonminimal solution to the SU(2) Yang-Mills Higgs equations on  $\mathbb{R}^{**3}$ , *Commun. Math. Phys.* **86**, 257 (1982).
- [42] Burkhard Kleihaus and Jutta Kunz, A monopole—anti-monopole solution of the SU(2) Yang-Mills-Higgs model, *Phys. Rev. D* **61**, 025003 (2000).
- [43] Moshe Israeli and Steven A. Orszag, Approximation of radiation boundary conditions, *J. Comput. Phys.* **41**, 115 (1981).